

Sandstone Composition in Ternary Plots

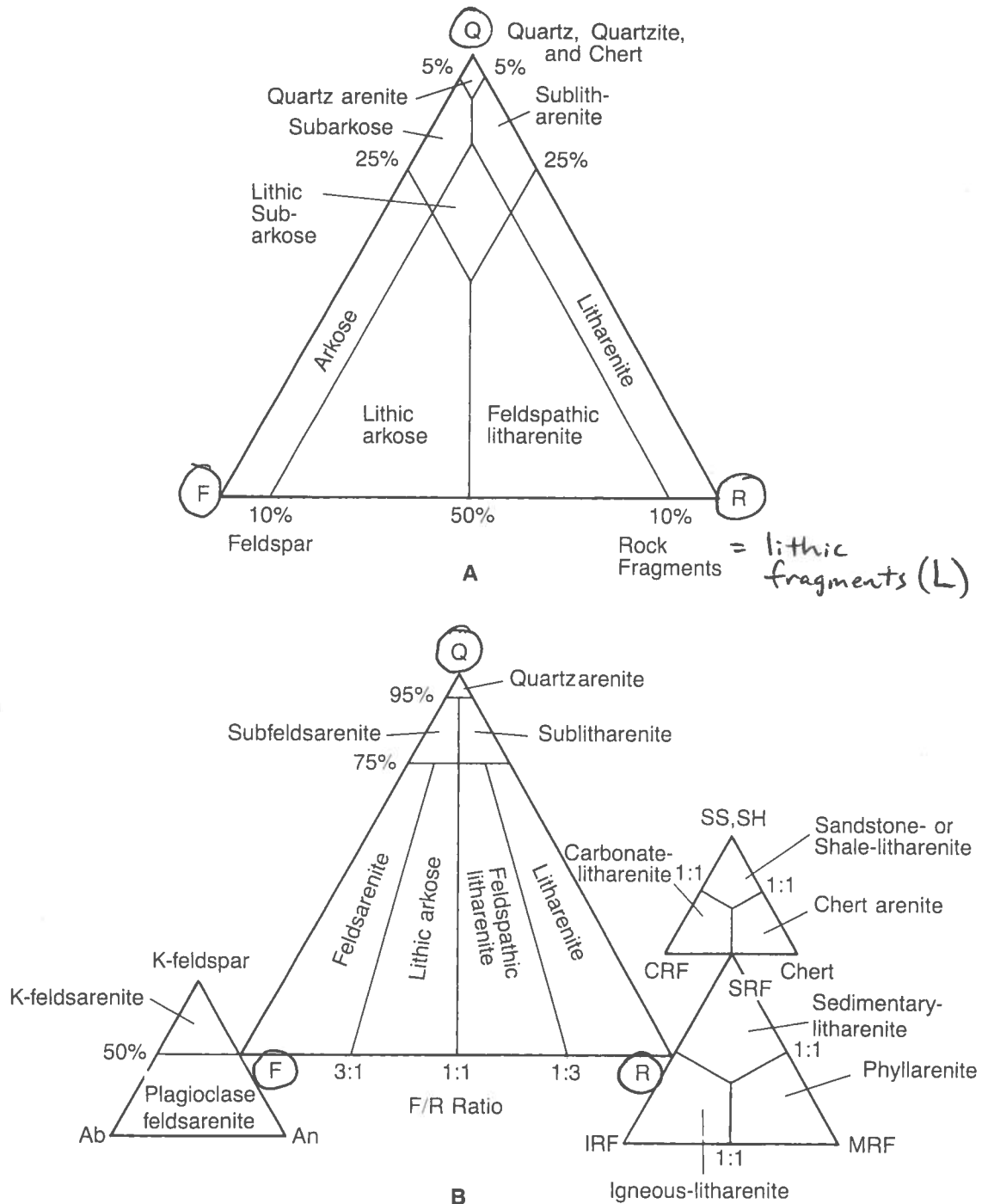
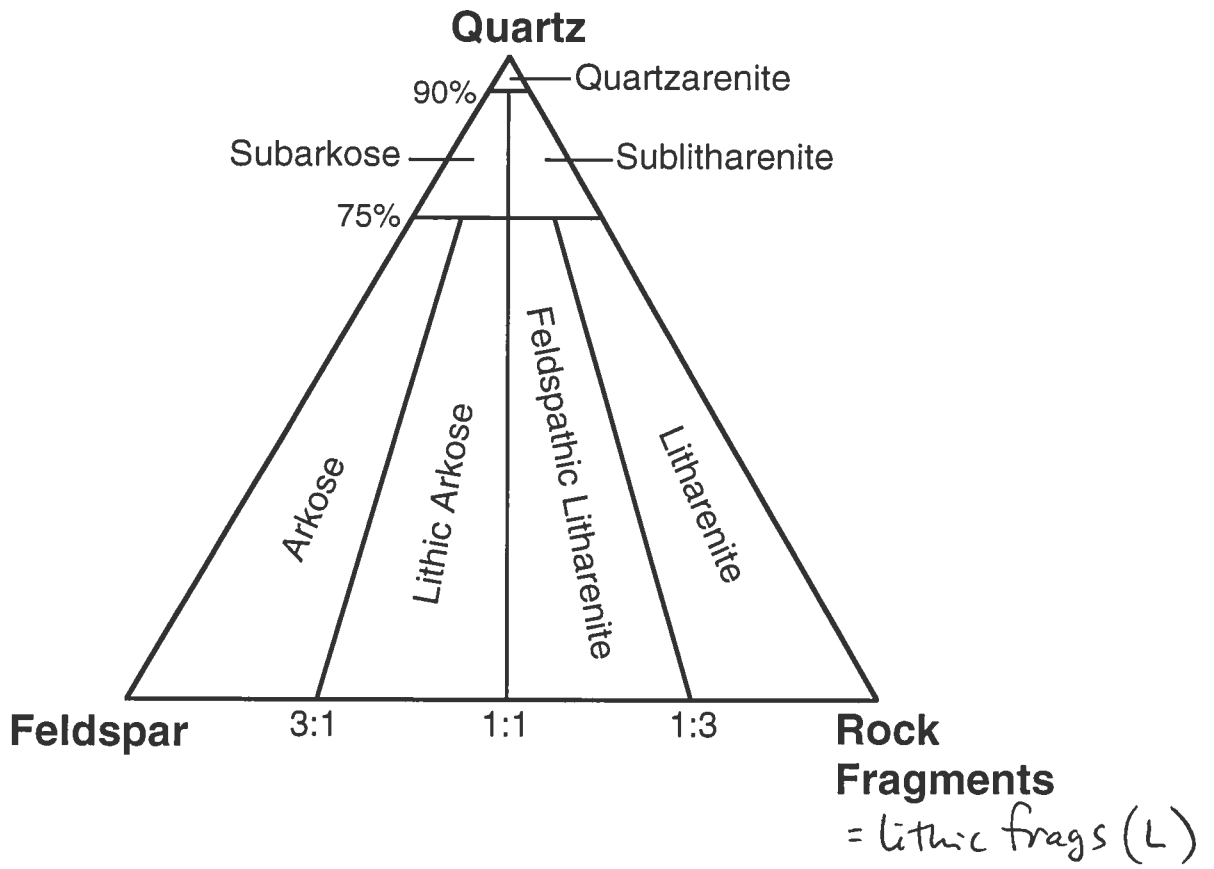


FIGURE 6.12 Classification of sandstones according to (A) McBride and (B) Folk, Andrews, and Lewis. In Folk et al.'s classification, chert is included with rock fragments at the R pole, and granite and gneiss fragments are included with feldspars at the F pole. SS = sandstone, SH = shale, CRF = carbonate rock fragments, SRF = sedimentary rock fragments, IRF = igneous rock fragments, MRF = metamorphic rock fragments (A, from McBride, E. F., 1963, A classification of common sandstones: *Jour. Sed. Petrology*, v. 34, Fig. 1, p. 667, reprinted by permission of Society of Economic Paleontologists and Mineralogists, Tulsa, Okla. B, from Folk, R. L., P. B. Andrews, and D. W. Lewis, 1970, Detrital sedimentary rock classification and nomenclature for use in New Zealand: *New Zealand Jour. of Geology and Geophysics*, v. 13, Fig. 8, p. 955, and Fig. 9, p. 959, British Crown copyright, reprinted by permission.)

Boggs (1995)



Modified Compositional Classification of Sandstones (Dorsey's fav.)

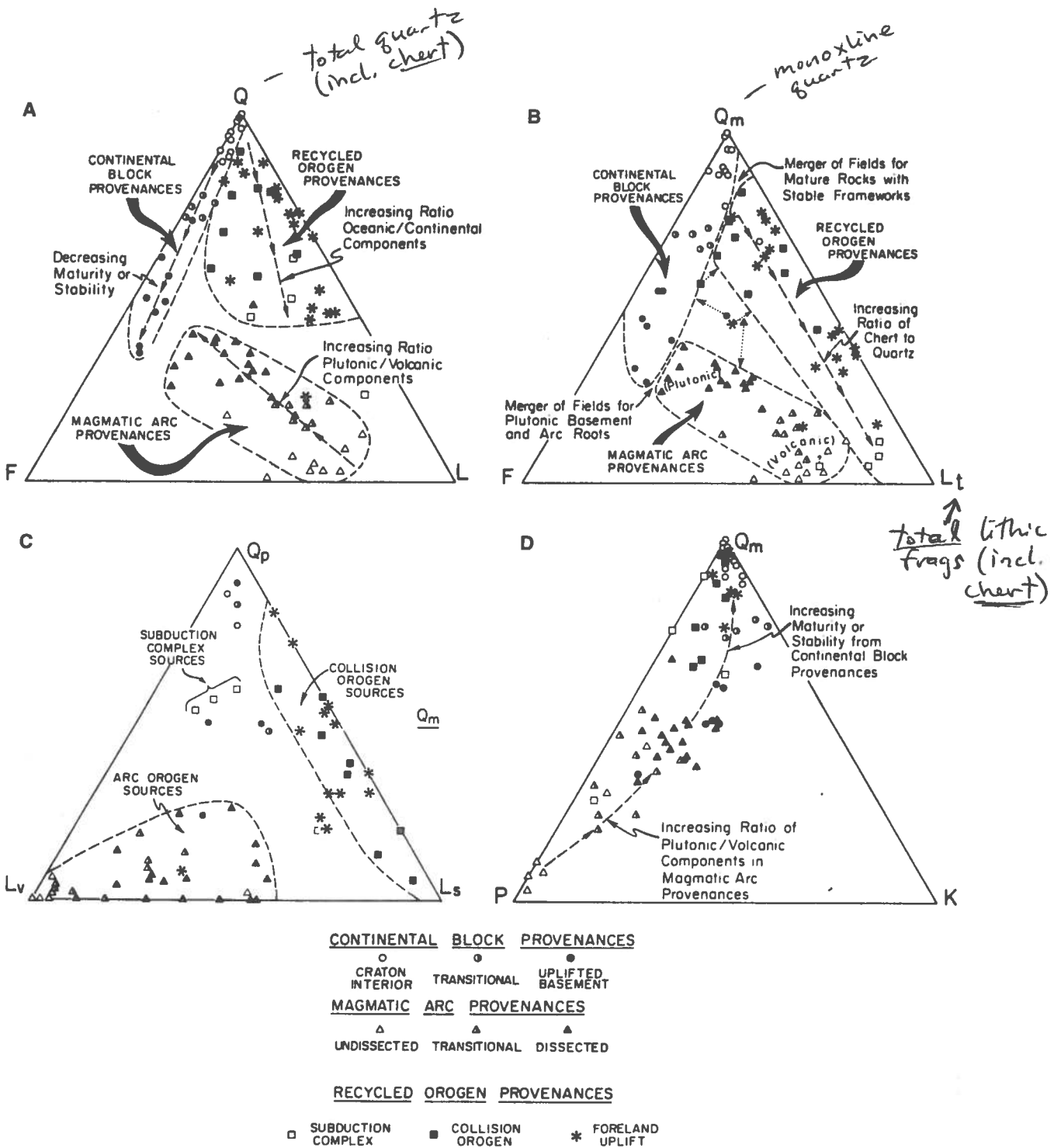


FIGURE 7.14 Four triangular plots showing mean framework modes (sand-size particle composition) for selected sandstone suites derived from different types of provenances: (A) QFL plot, (B) Q_mFL_t plot, (C) $Q_pL_vL_s$ plot, (D) Q_mPK plot. Q is total quartz, including monocrystalline (Q_m) and polycrystalline (Q_p) varieties, F is total feldspar grains, P is plagioclase feldspar grains, K is K-feldspar grains, L_t is total rock fragments, including stable quartzose (Q_p) and unstable (L) varieties, L_v is volcanic-metavolcanic rock fragments, and L_s is sedimentary-metasedimentary rock fragments. (After Dickinson, W. R., and C. A. Suczek, 1979, Plate tectonics and sandstone composition: Am. Assoc. Petroleum Geologists Bull., v. 63, Figs. 1-4, pp. 2171, 2172, reprinted by permission of AAPG, Tulsa, Okla.)

Bo995 (1987)

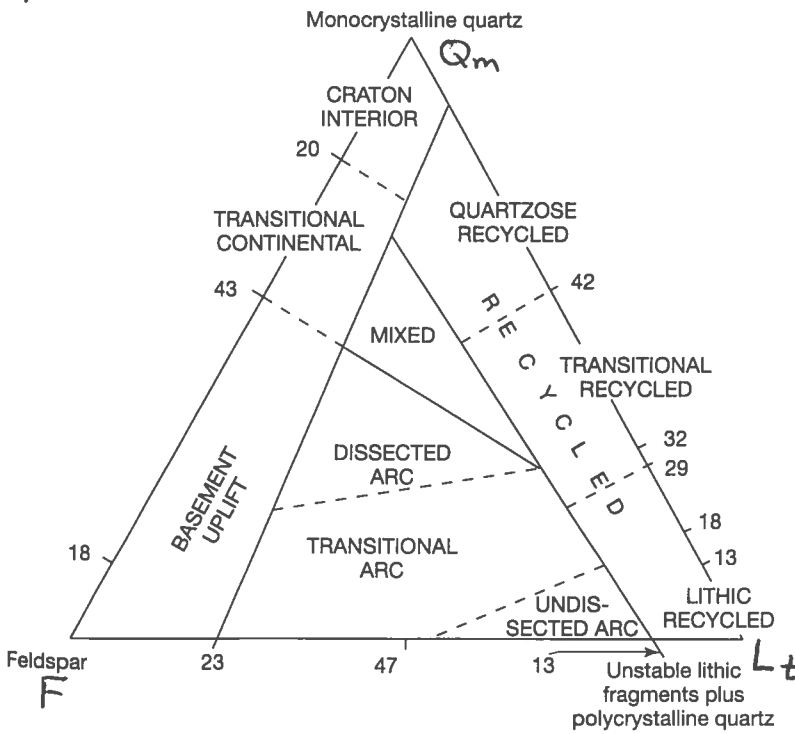
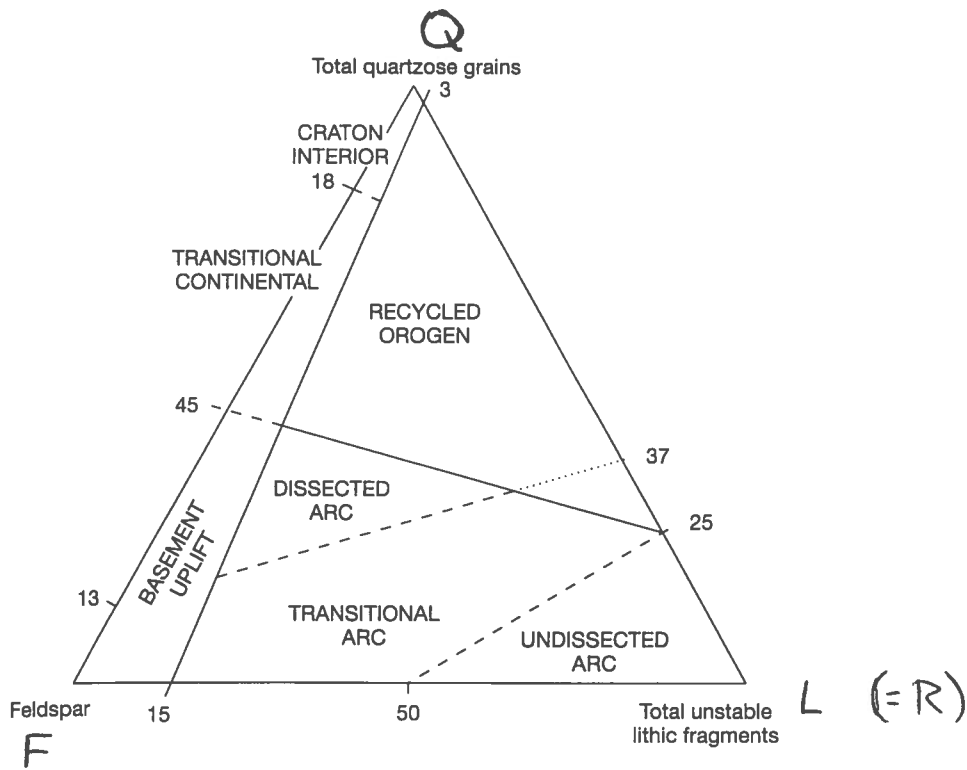


Figure 5.14
Relationship between framework composition of sandstones and tectonic setting. [After Dickinson, R. W., et al., 1983, Provenance of North American Phanerozoic sandstones in relation to tectonic setting: Geol. Soc. America Bull., v. 94, Fig. 1, p. 223. Reproduced by permission.]

Bo995 (2001)

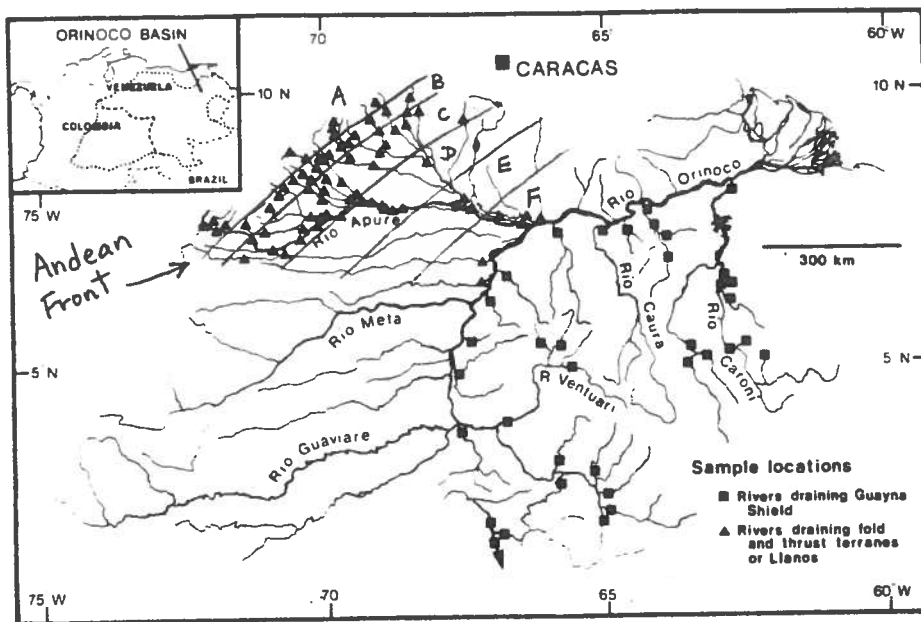


FIG. 2.—Major streams in the Orinoco drainage basin and locations of samples discussed in this paper.

- A. Samples from within the fold and thrust terranes (7 samples)
- B. Samples from the vicinity of the Andean front, the boundary between the Llanos and the fold and thrust terranes (22 samples)
- C. Samples from within 100 km of the Andean front (27 samples)
- D. Samples from 100-200 km of the Andean front (10 samples)
- E. Samples from 200-300 km of the Andean front (3 samples)
- F. Samples from rivers draining the western Llanos but not extending into the fold and thrust terranes (3 samples)

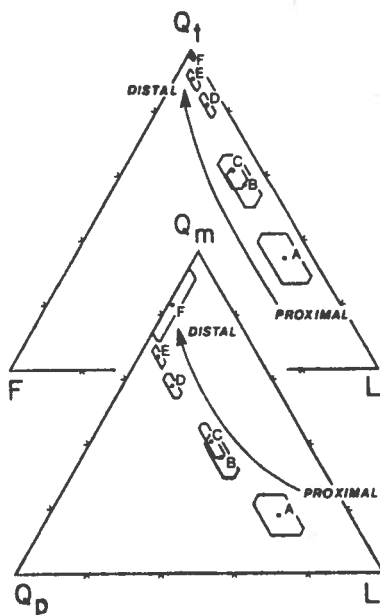


FIG. 8.—Qt-F-L (top) and Qm-Qp-L (bottom) compositional diagrams for sands from rivers in the Apure drainage. Axes ticks are at intervals of 20%. Suite means are plotted for each of the groupings of Andean-derived sands described in table 1. Error polygons enclose two standard errors of the mean (~95% confidence interval).

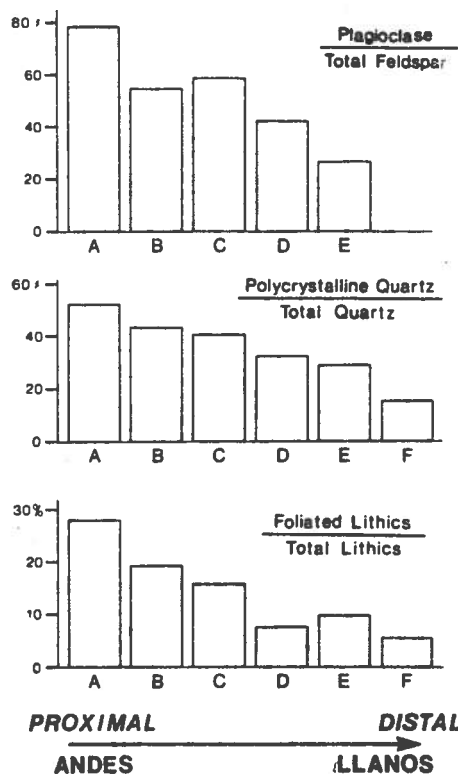


FIG. 9.—Histograms showing mean ratios of plagioclase to total feldspar (top), polycrystalline quartz to total quartz (middle), and foliated lithic fragments (including polycrystalline quartz) to total lithic fragments (bottom) for each of the groupings of Andean-derived sands described in table 1.

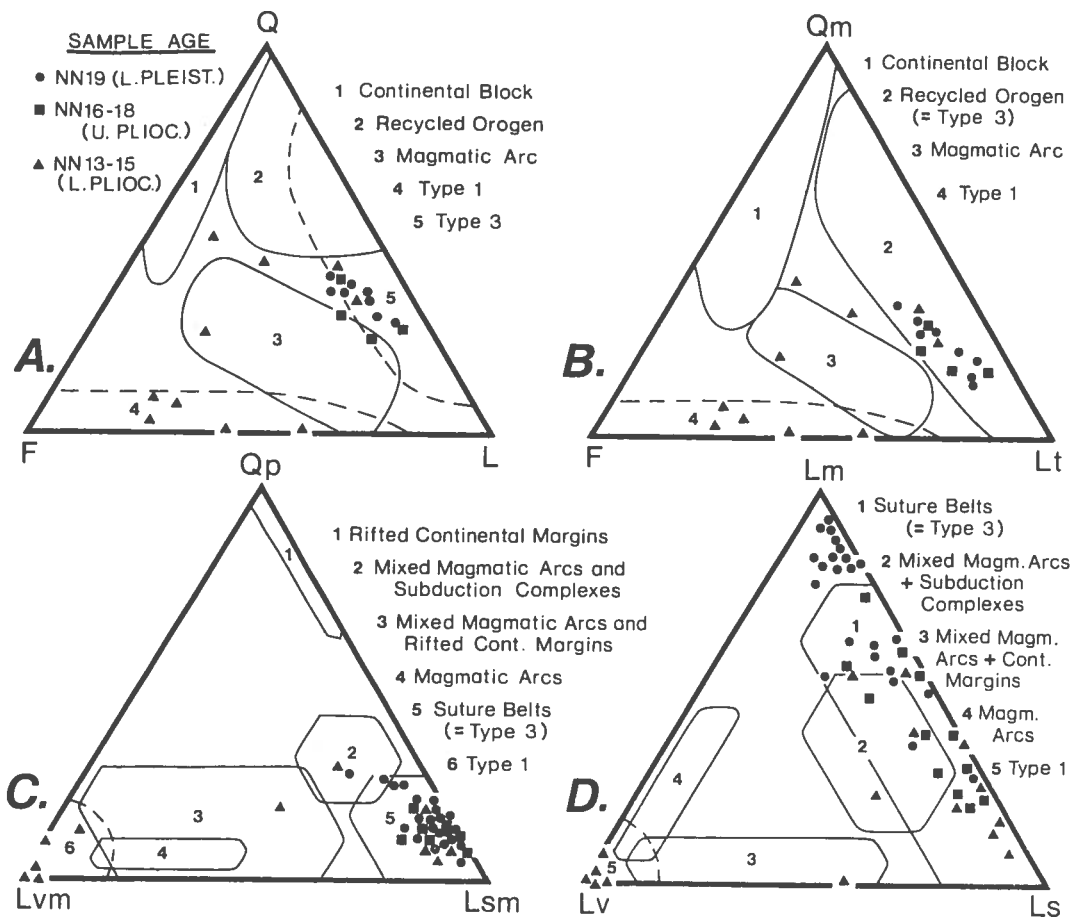


FIG. 5.—Ternary diagrams of Coastal Range sandstones. A (QFL) and B (QmFLt) are from Dorsey (1985a); C (QpLvmLsm) and D (LmLvLs) plot data from Dorsey (1985a) and this study. Provenance fields are from Dickinson and Suczek (1979) and Ingersoll and Suczek (1979); Type 1 and Type 3 are from Teng (1979). In general, the data fall into two clusters: 1) quartz-poor, feldspar-rich sandstones with abundant volcanic lithic fragments, all early Pliocene in age; and 2) feldspar- and volcanic-fragment-poor lithic arenites, ranging in age from early Pliocene to early Pleistocene, which contain moderate amounts of quartz and abundant sedimentary-metasedimentary lithic fragments. The age and compositional grouping represents a shift in source areas from the Luzon volcanic arc to the proto-Taiwan accretionary wedge that resulted from the early Pliocene onset of arc-continent collision (see Fig. 7).

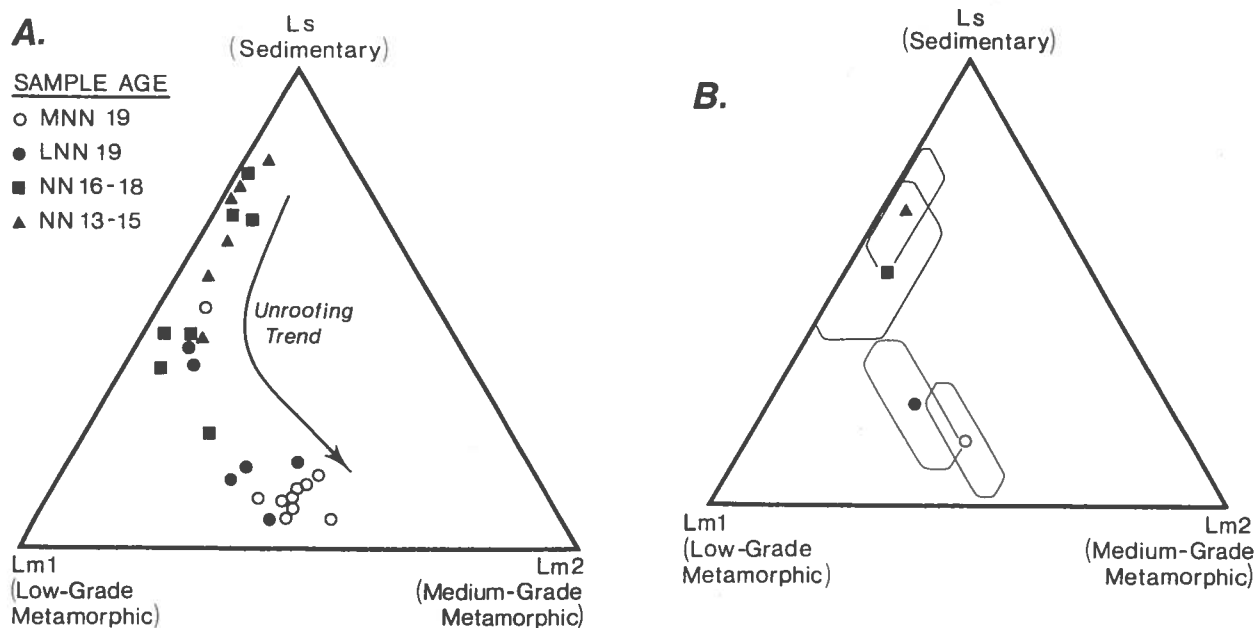


FIG. 6.—Ternary diagram of lithic fragments defined in this paper: sedimentary (Ls); low-grade metamorphic (Lm1); and medium-grade metamorphic (Lm2). A) Distribution of sandstones within a well-defined compositional field. Note that the oldest samples plot near the Ls corner, and younger samples become progressively enriched first in Lm1 and later in Lm2. B) Same diagram plotting means and standard deviations of each age group. Note the strong age dependence of the compositional trend; this reflects unroofing of the (meta)sedimentary complex through time and erosion into progressively deeper (higher-grade) levels in the collision belt.

Dorsey (1988) Jour. Sed. Petrology
v. 58 p. 208-218